Spin-wave study of the magnetic excitations in sandwich structures coupled by bilinear and biquadratic interlayer exchange

Monica Macciò and Maria Gloria Pini
Istituto di Elettronica Quantistica, Consiglio Nazionale delle Ricerche, I-50127 Firenze, Italy

Paolo Politi and Angelo Rettori
Dipartimento di Fisica, Universitá di Firenze, I-50125 Firenze, Italy

(Received 15 July 1993)

Using a microscopic and quantum approach, we study the ground-state configuration and the spin-wave excitations of a model of two ferromagnetic monolayers, interacting via both bilinear and biquadratic exchange, and subject to an easy-plane anisotropy, a quartic in-plane anisotropy and an external field. In the framework of a Green's-function method, we obtain analytical results for the spin-wave dispersion curves. Peculiar features are found in the field dependence of the acoustic and optical frequency gaps, in correspondence to the critical fields for which the canting angle between the magnetizations of the two coupled layers presents discontinuities. In particular, a minimum for the optical gap at the saturation field is predicted, which could be experimentally observed by Brillouin light scattering in real systems.

I. INTRODUCTION

Sandwich and superlattice structures consisting of ultrathin ferromagnetic films separated by nonmagnetic spacers have attracted much attention in recent years, both from the experimental[1–8] and theoretical [9–18] point of view. In their seminal work, Grünberg *et al.*[1] found evidence for antiferromagnetic coupling between Fe layers in a Fe/Cr/Fe sandwich by means of Brillouin light scattering (BLS). Later on, Parkin, More, and Roche[2] reported the observation of oscillations in exchange coupling and magnetoresistance in metallic superlattice structures as a function of the nonferromagnetic spacer thickness.

Recently, sandwich Fe/Cr/Fe structures with a wedge-shaped spacer were grown to investigate the sign and magnitude of the interlayer exchange in more detail. In these epitaxially grown samples, short period oscillations superimposed onto the long period ones were observed, both using scanning electron microscopy with polarization analysis[3] and Brillouin light scattering.[4]

Moreover, in the transition region between ranges of ferromagnetic and antiferromagnetic bilinear coupling, unusual domain patterns were observed by magnetooptic techniques,[5] and characteristic steps at half saturation were displayed by the easy axis magnetization curves, measured by magneto-optical Kerr effect.[5,6]

Such unusual features were attributed[5] to a canting between the magnetization directions of the two Fe slabs, which cannot be explained in terms of a conventional—ferromagnetic or antiferromagnetic—bilinear coupling between layers. Assuming a biquadratic interlayer exchange and treating the spins in the classical approximation, the field dependence of the $T=0$ magnetization was calculated in a numerical way.[5] The canting angle was found to depend on the size of the bilinear and biquadratic exchange constants and the experimentally observed preference for coupling angles near $\pi/2$ was accounted for including a cubic anisotropy in the model. Treating the magnetic structure as a continuum, one can also calculate[7] the long-wavelength ($q<10^5$ cm^{-1}) spin-wave energies, experimentally accessible by the light-scattering technique.

More recently, also ferromagnetic resonance and surface magneto-optical Kerr effect measurements in Fe/Cu/Fe trilayers[7] provided evidence for the simultaneous presence of bilinear and biquadratic exchange coupling between the magnetic layers.

An explanation for the physical origin of the biquadratic coupling[19] in such systems was proposed by Slonczewski,[15] in terms of a competition between ferromagnetic and antiferromagnetic bilinear coupling in the presence of interface roughness (atomic steps). Within this approach, the biquadratic coupling is not of microscopic origin, but arises from spatial fluctuations of the microscopically bilinear coupling, caused by terraced thickness fluctuations, at the monolayer scale, of the nonmagnetic spacer. Numerical calculations by Ribas and Dieny[16] confirmed Slonczewski's model in the limit of small terraces and small deviations of the angle between the ferromagnetic layers around $\pi/2$.

Subsequently, Barnaś and Grünberg[17,18] suggested two possible *microscopic* mechanisms, both of which give nonvanishing biquadratic coupling even for ideally flat interfaces. The first one is based on the assumption of bilinear exchange coupling between next-nearest-neighbor atomic planes in addition to the nearest-neighbor ones: The biquadratic term then appears as a result of the competition between interlayer and intralayer exchange couplings. The second mechanism is based on the fact that the electronic wave functions responsible for the coupling depend on the relative orientations of the film magnetizations.

This experimental and theoretical background induced us to study, within a microscopic and quantum approach, the ground-state configuration and the spin-wave excitations for a model of two ferromagnetic monolayers, interacting via both bilinear and biquadratic interlayer exchange and subject to an easy-plane single-ion anisotropy, a quartic in-plane anisotropy, and an external field. Whatever its origin, in our model the biquadratic coupling is assumed as a phenomenological parameter. In fact, our purpose is to study the dispersion curves of the spin-wave excitations with respect to the canted ground state, in order to have a method for determining the values of the bilinear and biquadratic interlayer exchange parameters.

We limit ourselves to the simplified case that each ferromagnetic film is made of only one monolayer, because this allows us to obtain analytical results for the frequencies of the two spin-wave modes of the system, and thus to control their dependence on the various Hamiltonian parameters.

Moreover, for the aim of describing the main features of Brillouin spectra, the results obtained by this simple model are expected to be valid also for sandwich structures consisting of two ultrathin ferromagnetic films, separated by a nonmagnetic spacer of fixed thickness, provided that the intralayer exchange coupling is much stronger than the interlayer one: in fact, in this case, the low-frequency modes measurable by Brillouin light scattering are determined by the feeble interlayer interactions.

Regarding the ground-state configuration, we find that the inclusion of quantum effects leads to some modifications in the boundaries of the $H=0$ phase diagram with respect to the classical case,[5] which is correctly recovered in the limit $S\rightarrow\infty$. We also study the field dependence of the mean of the magnetizations of the two coupled films at $T=0$ and find changes in its slope at the critical values of the field, for which the canting angle presents discontinuities.

Also the frequencies of the spin-wave excitations show peculiar features in their field dependence, in correspondence to such critical fields. In particular, the gap of the optical mode goes to zero for the value of the field at which the magnetization becomes saturated. By inspection of the analytic expression obtained for the gap, one can easily interpret this feature as due to the competition between the in-plane magnetic field and the in-plane fourfold anisotropy.

The layout of the paper is as follows: In Sec. II we present the model and find the ground-state configuration, both in zero and in an applied magnetic field. Section III is devoted to the calculation of the spin-wave modes of the system by means of a Green's-function method. In Sec. IV, the results are presented and discussed. Finally, we draw the conclusions in Sec. V.

II. THE MODEL AND THE GROUND-STATE CONFIGURATION

We assume the spins to be localized on the sites of two parallel monolayers, separated by a fixed distance c (the thickness of the nonmagnetic spacer) along the $y=[010]$ direction (the normal to the film plane). Each ferromagnetic monolayer is assumed to have a simple quadratic lattice structure, with lattice constant a. The interface between the two ferromagnetic monolayers is a registered (010) one. The spin Hamiltonian reads

$$\mathcal{H}=\mathcal{H}_1+\mathcal{H}_2\ , \tag{1}$$

where the explicit expression for $\mathcal{H}_1$ is

$$\mathcal{H}_1=-\frac{J}{2}\sum_{l_\parallel,\delta_\parallel}\mathbf{S}_1(l_\parallel)\cdot\mathbf{S}_1(l_\parallel+\delta_\parallel)-\frac{A}{2}\sum_{l_\parallel}\mathbf{S}_1(l_\parallel)\cdot\mathbf{S}_2(l_\parallel)-\frac{B}{2}\sum_{l_\parallel}[\mathbf{S}_1(l_\parallel)\cdot\mathbf{S}_2(l_\parallel)]^2+D\sum_{l_\parallel}[S_1^y(l_\parallel)]^2$$
$$-\frac{K}{2}\sum_{l_\parallel}\{[S_1^x(l_\parallel)]^4+[S_1^z(l_\parallel)]^4\}-\varepsilon\frac{K}{2}\sum_{l_\parallel}[S_1^y(l_\parallel)]^4-g\mu_B H\sum_{l_\parallel}[S_1^x(l_\parallel)\sin\psi+S_1^z(l_\parallel)\cos\psi]\ . \tag{2}$$

The $l_\parallel$ summation runs over the $N_\parallel$ sites of the simple quadratic lattice and the $\delta_\parallel$ summation runs over the four nearest neighbors, within the monolayer plane, of a given site. $\mathcal{H}_2$ is obtained from $\mathcal{H}_1$ by interchanging $\mathbf{S}_1$ and $\mathbf{S}_2$.

We are particularly interested in the peculiar features (e.g., a canted ground state) arising from the competition between a ferromagnetic intralayer exchange ($J>0$), a bilinear interlayer exchange (ferromagnetic, $A>0$, or antiferromagnetic, $A<0$) and an antiferromagnetic ($B<0$) biquadratic interlayer exchange. In real systems, the character (ferro- versus antiferromagnetic) and the intensity of the interlayer exchange depend on c, the thickness of the nonmagnetic spacer.[4–6] In our model, A and B are assumed as phenomenological parameters, i.e., we fix c and consequently the sign and the value of the interlayer exchange constants. We also consider an easy-plane anisotropy ($D>0$), favoring the spins to lie in the xz plane, and an anisotropy ($K>0$), which in the bulk case, $\varepsilon=1$, would have cubic symmetry. In the case of two coupled films, owing to the reduced symmetry of the system in the y direction, we assume $\varepsilon=0$, so that the in-plane anisotropy K favors the alignment of the spins along one of the four equivalent crystallographic directions [100], [$\bar{1}$00], [001], [00$\bar{1}$]. We also assume an external magnetic field to be applied within the easy plane, along a direction which forms an angle ψ with respect to the $z=[001]$ axis.

Denoting by φ_l the angle formed by the spin $\mathbf{S}_l(l_\parallel)$ with respect to the z direction, the relation between the spin components in the crystallographic frame of reference (with axes x,y,z) and the spin components in the local frame (with axes ξ,η,ζ) is

$$\begin{pmatrix} S_l^x(\mathbf{l}_\parallel) \\ S_l^y(\mathbf{l}_\parallel) \\ S_l^z(\mathbf{l}_\parallel) \end{pmatrix} = \begin{pmatrix} \cos\varphi_l & 0 & \sin\varphi_l \\ 0 & 1 & 0 \\ -\sin\varphi_l & 0 & \cos\varphi_l \end{pmatrix} \begin{pmatrix} S_l^\xi(\mathbf{l}_\parallel) \\ S_l^\eta(\mathbf{l}_\parallel) \\ S_l^\zeta(\mathbf{l}_\parallel) \end{pmatrix} . \quad (3)$$

In the framework of the spin-wave approximation, valid at temperatures low with respect to the Curie point, we express the spin operators in terms of bosonic creation and destruction operators via the Dyson-Maleev transformation[20] (ζ= quantization axis)

$$\begin{aligned} S_l^+(\mathbf{l}_\parallel) &= S_l^\xi(\mathbf{l}_\parallel) + iS_l^\eta(\mathbf{l}_\parallel) \\ &= \sqrt{2S}\left[1 - \frac{1}{2S} a_l^\dagger(\mathbf{l}_\parallel) a_l(\mathbf{l}_\parallel)\right] a_l(\mathbf{l}_\parallel) , \\ S_l^-(\mathbf{l}_\parallel) &= S_l^\xi(\mathbf{l}_\parallel) - iS_l^\eta(\mathbf{l}_\parallel) \\ &= \sqrt{2S}\, a_l^\dagger(\mathbf{l}_\parallel) , \\ S_l^\zeta(\mathbf{l}_\parallel) &= S - a_l^+(\mathbf{l}_\parallel) a_l(\mathbf{l}_\parallel) . \end{aligned} \quad (4)$$

Applying the transformations (3) and (4) to the spin Hamiltonian (1), performing the normal ordering of the bosonic operators, and retaining up to the quadratic terms in $a^\dagger$ and a, one obtains

$$\mathcal{H} = E^0 + \mathcal{H}^{(1)} + \mathcal{H}^{(2)} , \quad (5)$$

where $E^{(0)}$, $\mathcal{H}^{(1)}$, and $\mathcal{H}^{(2)}$ denote the parts of the boson Hamiltonian containing zero, one, and two boson operators, respectively.

The constant part $E^{(0)}$ is given by

$$E^{(0)} = E_c + E(\varphi_1, \varphi_2) , \quad (6)$$

where

$$\begin{aligned} E_c/N_\parallel &= -4JS^2 - BS^2\left[S + \frac{1}{4}\right] + DS \\ &\quad - KS^2\left[S^2 + (1-\varepsilon)\left[\frac{3}{4} - \frac{1}{4S}\right]\right] , \end{aligned} \quad (7)$$

$$\begin{aligned} E(\varphi_1, \varphi_2)/N_\parallel &= -[AS^2 - \tfrac{1}{2}BS^2]\cos(\varphi_2 - \varphi_1) \\ &\quad - BS^4 f_s^2 \cos^2(\varphi_2 - \varphi_1) \\ &\quad + \tfrac{1}{4}KS^4 g_s [\sin^2(2\varphi_1) + \sin^2(2\varphi_2)] \\ &\quad - g\mu_B HS[\cos(\psi - \varphi_1) + \cos(\psi - \varphi_2)] , \end{aligned} \quad (8)$$

and we have defined

$$f_s \equiv \left[1 - \frac{1}{2S}\right] \quad g_s \equiv \left[1 - \frac{1}{2S}\right]\left[1 - \frac{1}{S}\right]\left[1 - \frac{3}{2S}\right] . \quad (9)$$

In the classical limit $S \to \infty$, both the factors f_s and g_s tend to 1; moreover, on the right-hand side of Eq. (8) one can neglect the terms in BS^2 and BS^3, coming from the normal ordering of the bosonic operators, with respect to BS^4. One thus recovers the classical result[5] for the ground-state energy.[21]

Depending on the actual values of the Hamiltonian parameters, either collinear or canted ground-state configurations are obtained from Eq. (8) by minimizing $E(\varphi_1, \varphi_2)$ with respect to φ_1 and φ_2. Equivalently, one can introduce the new variables $\varphi_+ = \varphi_2 + \varphi_1$ and $\varphi_- = \varphi_2 - \varphi_1$, in terms of which the ground-state energy $E(\varphi_1, \varphi_2)$ is expressed as

$$\begin{aligned} E(\varphi_+, \varphi_-)/N_\parallel &= -[AS^2 - \tfrac{1}{2}BS^2] \\ &\quad \times \cos(\varphi_-) - BS^4 f_s^2 \cos^2(\varphi_-) \\ &\quad + \tfrac{1}{4}KS^4 g_s [1 - \cos(2\varphi_-)\cos(2\varphi_+)] \\ &\quad - 2g\mu_B HS \cos\left[\frac{\varphi_-}{2}\right] \cos\left[\psi - \frac{\varphi_+}{2}\right] . \end{aligned} \quad (10)$$

The conditions for an extremum are

$$\begin{aligned} \frac{\partial E(\varphi_+, \varphi_-)}{\partial \varphi_-} &= 0 = [AS^2 - \tfrac{1}{2}BS^2]\sin(\varphi_-) \\ &\quad + 2BS^4 f_s^2 \sin(\varphi_-)\cos(\varphi_-) \\ &\quad + \tfrac{1}{2}KS^4 g_s \sin(2\varphi_-)\cos(2\varphi_+) \\ &\quad + g\mu_B HS \sin\left[\frac{\varphi_-}{2}\right]\cos\left[\psi - \frac{\varphi_+}{2}\right] , \end{aligned} \quad (11a)$$

$$\begin{aligned} \frac{\partial E(\varphi_+, \varphi_-)}{\partial \varphi_+} &= 0 = \tfrac{1}{2}KS^4 g_s \cos(2\varphi_-)\sin(2\varphi_+) \\ &\quad - g\mu_B HS \cos\left[\frac{\varphi_-}{2}\right]\sin\left[\psi - \frac{\varphi_+}{2}\right] . \end{aligned} \quad (11b)$$

A. $H = 0$ case

Let us first consider the ground-state configuration in the absence of an external field. For $H = 0$, Eq. (11b) is satisfied either by $\cos(2\varphi_-) = 0$ or by $\sin(2\varphi_+) = 0$. Examining the second derivatives, one can easily see that the former solution corresponds to a maximum, whilst the minima are obtained solving Eq. (11a) with $\cos(2\varphi_+) = \pm 1$. Four different ground-state configurations are found.

(1) A ferromagnetic (F) ground state, characterized by $\cos(\varphi_-) = 1$, is obtained, for $\sin(\varphi_-) = 0$ and $\cos(2\varphi_+) = 1$, provided that $2A + 4BS(S-1) + 2KS^2 g_s > 0$.

(1) An antiferromagnetic (AF) ground state, characterized by $\cos(\varphi_-) = -1$, is obtained, for $\sin(\varphi_-) = 0$ and $\cos(2\varphi_+) = 1$, provided that

$$-2A + 2B(2S^2 - 2S + 1) + 2KS^2 g_s > 0 .$$

(3) A canted ground state (B), characterized by

$$\cos(\varphi_-) = \frac{2A - B}{-2KS^2 g_s - 4BS^2 f_s^2} \quad (12a)$$

is obtained, for $\cos(2\varphi_+)=1$, provided that $1/\sqrt{2}<|\cos(\varphi_-)|<1$ and $-2KS^2g_2-4BS^2f_s^2>0$. In Fig. 1 this canted ground state corresponds to the region between f_1 and f_3.

(4) A canted ground state (C), characterized by

$$\cos(\varphi_-)=\frac{2A-B}{2KS^2g_s-4BS^2f_s^2} \tag{12b}$$

is obtained, for $\cos(2\varphi_+)=-1$, provided that $|\cos(\varphi_-)|<1/\sqrt{2}$ and $2KS^2g_s-4BS^2f_s^2>0$.

In the classical limit $S\rightarrow\infty$, one recovers the results previously found in Ref. 5 for the ground-state configurations in zero field. Owing to the inclusion of quantum effects, we find some modifications in the phase boundaries with respect to the classical case: see Fig. 1, where the phase diagram in zero field is shown for $S=2$. The analytic expressions for the various phase lines are reported in the Appendix. Here we only observe that the curves f_0 for $\alpha<0$ (where $\alpha\equiv A/K$ and $\beta\equiv B/K$) and f_1 for any α are of second order, whilst all the other ones are of first order.

First, it should be noted that the canted ground-state configuration of type B, not studied in Ref. 5 because of a more limited range of parameters, is possible only for high values of the ratio α and β. Since the interesting range, for the purpose of studying coupled ultrathin films, corresponds to small values of α, in the following we will limit ourselves to consider the canted ground state of type C (and the excitations with respect to it). However, the most striking effect, due to the inclusion of quantum corrections, is an asymmetry in the phase boundaries for a reflection with respect to the $\alpha=0$ axis.[22] This leads to the possibility—quite unexpected within a classical approach—of having an antiferromagnetic ground state even for $A>0$. Such a feature is clearly a consequence of the quantum treatment of the biquadratic exchange in the model.

B. $H\neq0$ case

It would be rather laborious, and beyond the scope of the present paper, to extend the phase diagram calculated for $H=0$ to the general case of finite field.[23] Here we limit ourselves to calculate the field dependence of the magnetization when the field is applied along a direction of high symmetry for the in-plane anisotropy K, i.e., along a hard axis (e.g., [101]), or an easy axis (e.g., [100]).

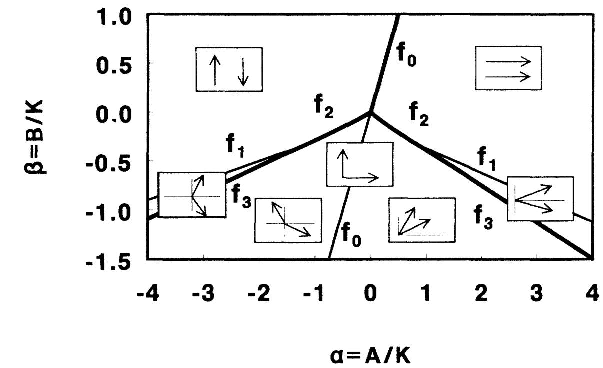

FIG. 1. Zero-field phase diagram for the ground state of a system made of two ferromagnetic monolayers, with a fourfold in-plane anisotropy (K), coupled via bilinear (A) and biquadratic (B) interplane exchange and with spin $S=2$. The insets show the different arrangements of the magnetizations in the two coupled films. The equations for the phase boundary lines are given in the Appendix. First- and second-order transition lines are denoted by heavy solid and light solid line-types, respectively.

1. *H along a hard axis*

Starting from a canted ground state of type C in zero field, let us now suppose to apply a magnetic field parallel to the film plane along a hard axis: $\psi=(2n+1)(\pi/4)(n=0,1,2,\ldots)$. Since, for $H=0$, the magnetizations of the two films are disposed symmetrically with respect to the hard axis (see Fig. 1), the effect of increasing the magnetic field will simply be to reduce the canting angle φ_-, while leaving φ_+ unchanged with respect to the $H=0$ case. For sufficiently high values of the field, a ferromagnetic ground state will be found, with the magnetizations of the two films completely aligned along the field direction. In conclusion, for H applied along a hard axis, by symmetry reasons one has $\cos(2\varphi_+)=-1$ and $\cos(\psi-\varphi_+/2)=1$, so that Eq. (11b) is satisfied and Eq. (11a) takes the form

$$\left\{\cos^3\left[\frac{\varphi_-}{2}\right]-\frac{1}{2}\left[1+\frac{2A-B}{2KS^2g_s-4BS^2f_s^2}\right]\cos\left[\frac{\varphi_-}{2}\right]-\frac{1}{2S}\frac{g\mu_BH}{2KS^2g_s-4BS^2f_s^2}\right\}\sin\left[\frac{\varphi_-}{2}\right]=0\ . \tag{13}$$

In the limit of zero field, it is immediate to solve Eq. (13), and the ferromagnetic (F), antiferromagnetic (AF) and canted (C) ground states discussed at the previous paragraph are correctly recovered. For $H\neq0$, the antiferromagnetic ground state is no more allowed. One finds either a canted ground state, when the term in braces in Eq. (13) vanishes, or a ferromagnetic one, when $\sin(\varphi_-/2)=0$. From the analysis of the second derivatives, one finds that the ferromagnetic ground state is favored provided that the field overcomes a critical value:

$$H>H_c=\frac{S}{g\mu_B}[-2A+B-4BS^2f_s^2+2KS^2g_s]\ .$$

From this equation it is clear that, when the field is applied along a hard axis, the quartic in-plane anisotropy K

opposes itself to the attainment of the ferromagnetic order.

In Fig. 2 we report the mean of the $T=0$ magnetizations of the two coupled films, $M/M_s=\cos(\varphi_-/2)$, ($M_s=$ saturation magnetization) as a function of the intensity of the magnetic field, applied along the hard axis. One finds that the saturation of the magnetization occurs just at the critical field H_c, for which the canting angle φ_- vanishes.

2. *H along an easy axis*

Starting from a canted ground state of type C in zero field, let us now suppose to apply a magnetic field parallel to the film plane along another direction of high symmetry, i.e., along an easy axis: $\psi=n(\pi/2)(n=0,1,2,\ldots)$. In this case, the ground-state configuration is determined by two independent variables: The canting angle φ_- and the angle $\Gamma=\varphi_+/2$ formed by the vector sum of the magnetizations in the two films with the field direction. Thus, for field applied along an easy axis, one has to solve a truly two-dimensional minimum problem, Eqs. (11a) and (11b), in order to find the ground-state configuration. In general, this can be done only numerically.

In Figs. 3(a)–3(c) we report the mean of the $T=0$ magnetizations of the two coupled films

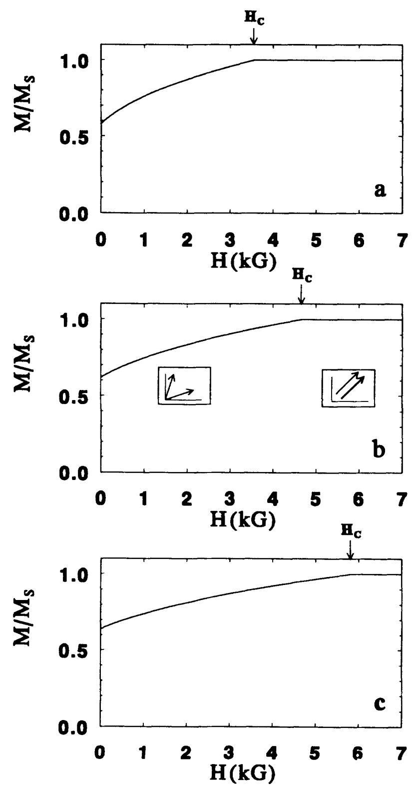

FIG. 2. Mean of the $T=0$ magnetizations of the two coupled films as a function of the intensity of a magnetic field, applied along an in-plane hard axis {101}, for selected values of the fourfold in-plane anisotropy K: (a) $K=0$; (b) $K=0.10$ K; (c) $K=0.20$ K. The other Hamiltonian parameters are fixed to $A=-0.04$ K; $B=-0.02$ K; $S=2$.

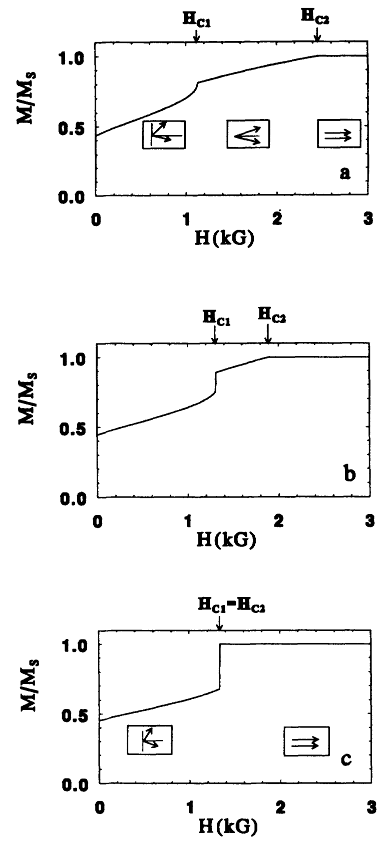

FIG. 3. Mean of the $T=0$ magnetizations of the two coupled films as a function of the intensity of a magnetic field, applied along an in-plane easy axis {001}, for selected values of the fourfold in-plane anisotropy K: (a) $K=0.10$ K; (b) $K=0.15$ K; (c) $K=0.20$ K. The other Hamiltonian parameters are the same as in Fig. 2.

$$\frac{M}{M_s}=\frac{1}{2}[\cos(\varphi_1)+\cos(\varphi_2)]$$

$$=\frac{1}{2}\left[\cos\left[\Gamma-\frac{\varphi_-}{2}\right]+\cos\left[\Gamma+\frac{\varphi_-}{2}\right]\right]$$

as a function of the intensity of the magnetic field, applied along the easy axis, for selected values of the in-plane anisotropy K.

In cases a and b, which refer to low values of K, two critical fields are found. In correspondence to the first one, H_{c1}, the angle Γ changes abruptly from a finite value to 0, while the canting φ_- is still finite. Thus, for $H>H_{c1}$ one has a highly symmetric canted ground-state configuration, with the magnetizations of the two layers forming opposite angles with the field direction. The saturation of the magnetization occurs at the second critical field

$$H_{c2}=\frac{S}{g\mu_B}[-2A+B-4BS^2f_s^2-2KS^2g_s]$$

($H_{c2}>H_{c1}$), for which also the canting angle φ_- becomes zero. Clearly, in the case of a field applied along the easy axis, the in-plane quartic anisotropy K favors the attainment of the ferromagnetic order.

In case c, corresponding to a higher value of K, only one critical field is found, $H_{c1} \equiv H_{c2}$, at which the angle Γ and the canting φ_- simultaneously change from a finite value to 0 in an abrupt manner.

It is worthwhile to observe that, for magnetic field applied along an easy axis, and for opportune thickness of the nonmagnetic spacer (corresponding in our model to opportune values of the interlayer exchange parameters), a field dependence of the magnetization very similar to that obtained in our Fig. 3(c) was observed in Fe/Cr/Fe trilayers [see Fig. 10(e) of Ref. 5], while in some Fe/Cu/Fe samples evidence was found for two critical fields [see Fig. 7(a) of Ref. 8], like those observed in our Figs. 3(a) and 3(b).

We conclude this paragraph by observing that the ground-state configuration could have also been obtained, in an equivalent way, from the one-boson Hamiltonian $\mathcal{H}^{(1)}$

$$\mathcal{H}^{(1)}=\frac{1}{\sqrt{2S}}\sum_{l_\parallel}(\{-[a_1(l_\parallel)+a_1^\dagger(l_\parallel)]+[a_2(l_\parallel)+a_2^\dagger(l_\parallel)]\}[AS^2-\tfrac{1}{2}BS^2+2BS^4f_s^2\cos(\varphi_2-\varphi_1)]\sin(\varphi_2-\varphi_1))$$
$$+\frac{1}{\sqrt{2S}}\sum_{l=1,2}\sum_{l_\parallel}\{[a_l(l_\parallel)+a_l^\dagger(l_\parallel)][\tfrac{1}{2}KS^4g_s\sin(4\varphi_l)-g\mu_B HS\sin(\psi-\varphi_l)]\}\ . \tag{14}$$

In fact, by requiring the coefficients of the one-boson terms ($[a_1+a_1^\dagger]$ and $[a_2+a_2^\dagger]$) in Eq. (14) to vanish, one recovers the two conditions for $E(\varphi_1,\varphi_2)$ to have an extremum. Reversely, one can easily verify that, in correspondence to the values of φ_1 and φ_2 which minimize the ground-state energy $E(\varphi_1,\varphi_2)$, the one-boson Hamiltonian $\mathcal{H}^{(1)}$ vanishes.

III. SPIN-WAVE FREQUENCIES

Performing the Fourier transformation[20] in the film plane, where translational invariance is preserved,

$$a_{\mathbf{k}_\parallel,l}^\dagger=\frac{1}{\sqrt{N_\parallel}}\sum_{l_\parallel}e^{i\mathbf{k}_\parallel\cdot l_\parallel}a_l^\dagger(l_\parallel)\ ,$$
$$a_{\mathbf{k}_\parallel,l}=\frac{1}{\sqrt{N_\parallel}}\sum_{l_\parallel}e^{-i\mathbf{k}_\parallel\cdot l_\parallel}a_l(l_\parallel)\ , \tag{15}$$

the two-boson Hamiltonian $\mathcal{H}^{(2)}$ takes the form

$$\mathcal{H}^{(2)}=\mathcal{H}_h^{(2)}+\mathcal{H}_{nh}^{(2)}\ . \tag{16}$$

The Hermitian part $\mathcal{H}_h^{(2)}$ of the bilinear Hamiltonian reads

$$\mathcal{H}_h^{(2)}=\sum_{l,m=1,2}\sum_{\mathbf{k}_\parallel}\{A_{lm}a_{\mathbf{k}_\parallel,l}^\dagger a_{\mathbf{k}_\parallel,m}+\tfrac{1}{2}B_{lm}(a_{\mathbf{k}_\parallel,l}^\dagger a_{-\mathbf{k}_\parallel,m}^\dagger+a_{\mathbf{k}_\parallel,l}a_{-\mathbf{k}_\parallel,m})\}\ , \tag{17}$$

where the diagonal elements are given by

$$A_{ll}=4JS[1-\gamma(\mathbf{k}_\parallel)]+g\mu_B H\cos(\psi-\varphi_l)+DSf_s+AS\cos(\varphi_2-\varphi_1)$$
$$-\tfrac{1}{4}BS[-3(2S-1)^2\cos^2(\varphi_2-\varphi_1)+2\cos(\varphi_2-\varphi_1)+(2S-1)^2]$$
$$-\tfrac{1}{4}K(2S-1)\{[-4S^2+7S-4+\varepsilon(3S-2)]+\tfrac{5}{2}(S-1)(2S-3)\sin^2(2\varphi_l)\}\ , \tag{18a}$$

$$B_{ll}=-DSf_s-\tfrac{1}{4}BS(2S-1)^2\sin^2(\varphi_2-\varphi_1)-\tfrac{1}{4}K(2S-1)[(3S-2)(1-\varepsilon)+\tfrac{3}{2}(S-1)(2S-3)\sin^2(2\varphi_l)]\ , \tag{18b}$$

and the off-diagonal ones ($l\neq m$) by

$$A_{lm}=A_{ml}=-\tfrac{1}{2}AS[1+\cos(\varphi_2-\varphi_1)]-\tfrac{1}{2}BS[(2S-1)^2\cos^2(\varphi_2-\varphi_1)+2S(S-1)\cos(\varphi_2-\varphi_1)+(-2S^2+2S-1)]\ , \tag{18c}$$

$$B_{lm}=B_{ml}=-\tfrac{1}{2}AS[\cos(\varphi_2-\varphi_1)-1]-\tfrac{1}{2}BS[(2S-1)^2\cos^2(\varphi_2-\varphi_1)+(-2S^2+2S-1)\cos(\varphi_2-\varphi_1)-2S(S-1)]\ . \tag{18d}$$

In Eqs. (18) one has $\gamma(\mathbf{k}_\parallel)=\frac{1}{2}[\cos(k_x a)+\cos(k_z a)]$, with $-\pi\le k_x a,k_z a\le+\pi$ and the angles φ_1, φ_2, and ψ depend on the type of ground-state configuration and on the direction of the magnetic field. Notice that in Eqs. (18) the kinematic consistency[24] is satisfied both by the easy-plane anisotropy D and the cubic anisotropy K in the case $\varepsilon=1$ (bulk anisotropy limit), since the former does not contribute to the energy of the excitations for $S=\frac{1}{2}$ and the latter for $S<2$.[25]

The non-Hermitian part $\mathcal{H}_{nh}^{(2)}$ of the two-boson Hamiltonian is

$$\mathcal{H}_{nh}^{(2)} = -\sum_{\mathbf{k}_\parallel}\sum_{l=1,2}(a^\dagger_{\mathbf{k}_\parallel,l}a^\dagger_{-\mathbf{k}_\parallel,l})\{\tfrac{1}{4}D+\tfrac{1}{4}BS(S-\tfrac{1}{2})\sin^2(\varphi_2-\varphi_1)+\tfrac{1}{8}K[(3S-2)(1-\varepsilon)+\tfrac{3}{2}(S-1)(2S-3)\sin^2(2\varphi_l)]\} . \quad (19)$$

From Eqs. (16) and (19) it appears that the bilinear bosonic Hamiltonian $\mathcal{H}^{(2)}$ is a non-Hermitian operator: This is a well-known drawback of the Dyson-Maleev transformation. Moreover, in the non-Hermitian part $\mathcal{H}_{nh}^{(2)}$, the kinematic consistency is not satisfied. Similar problems, related to the use of the Dyson-Maleev transformation, were found in the study of the magnon spectrum of a Heisenberg ferromagnet with easy-plane anisotropy. In that case, Rastelli and Tassi[26] performed a generalized Bogoliubov[20] transformation in order to diagonalize the Hermitian, kinematically consistent part of the bosonic bilinear Hamiltonian; treating all the remaining as a perturbation, they were able to prove that the $T=0$ magnon spectrum satisfies the Goldstone theorem[27] [i.e., $\omega(k)\to 0$ for $k\to 0$] and is kinematically consistent (i.e., the easy-plane anisotropy does not contribute to the energy of the excitations for $S=\frac{1}{2}$) within terms of the order $[D/2JSz]^2 f_s^2$. We assume that also in the more complicated case under study, the Hermitian and kinematically consistent part of the bilinear Hamiltonian $\mathcal{H}_h^{(2)}$ should be a good starting point for a perturbative expansion, but we do not perform it explicitly.

In order to find the normal modes of the Hamiltonian (17), we will use a Green's-function formalism, previously developed for the study of magnetic films.[28] We define the Fourier transformed retarded Green's functions

$$G_{lm}(\mathbf{k}_\parallel,E) = \langle\langle a_{\mathbf{k}_\parallel,l};a^\dagger_{\mathbf{k}_\parallel,m}\rangle\rangle_E ,$$
$$G'_{lm}(\mathbf{k}_\parallel,E) = \langle\langle a^\dagger_{-\mathbf{k}_\parallel,l};a^\dagger_{\mathbf{k}_\parallel,m}\rangle\rangle_E . \quad (20)$$

Writing their equations of motion, the spin-wave frequencies are obtained from the poles of the Green's functions as the eigenvalues of the nonsymmetric 4×4 real matrix

$$\mathcal{T}(\mathbf{k}_\parallel) = \begin{pmatrix} A_{11} & A_{12} & B_{11} & B_{12} \\ A_{21} & A_{22} & B_{21} & B_{22} \\ -B_{11} & -B_{12} & -A_{11} & -A_{12} \\ -B_{21} & -B_{22} & -A_{21} & -A_{22} \end{pmatrix} , \quad (21)$$

where the elements of the dynamical matrix $\mathcal{T}(\mathbf{k}_\parallel)$ are defined by Eqs. (18). It is worthwhile to notice that, since $\mathcal{T}(\mathbf{k}_\parallel)$ and $\mathcal{T}(-\mathbf{k}_\parallel)$ have the same eigenvalues, half of them are positive and half negative, with the same absolute value. This is a well-known feature[28] of the energy spectrum of a nondiagonal bilinear Hamiltonian, such as (17).

The dispersion relations of the magnetic excitations are found solving a biquadratic equation and turn out to be

$$\omega_\pm^2(\mathbf{k}_\parallel) = \left[\frac{A_{11}^2+A_{22}^2}{2}-\frac{B_{11}^2+B_{22}^2}{2}+(A_{12}^2-B_{12}^2)\right]$$
$$\pm\left\{\left[\frac{A_{11}^2-A_{22}^2}{2}-\frac{B_{11}^2-B_{22}^2}{2}\right]^2+[A_{12}(A_{11}+A_{22})-B_{12}(B_{11}+B_{22})]^2 -[A_{12}(B_{11}-B_{22})-B_{12}(A_{11}-A_{22})]^2\right\}^{1/2} . \quad (22)$$

It is interesting to find the explicit expressions for the spin-wave frequencies in some limiting cases with high symmetry, such that $A_{11}=A_{22}$ and $B_{11}=B_{22}$.

A. $H=0$ case

In the absence of an external field, we suppose the ground-state configuration to be a canted one of type C. Thus, by symmetry reasons one has $\sin^2(2\varphi_1)=\sin^2(2\varphi_2)$, so that $A_{11}=A_{22}$ and $B_{11}=B_{22}$.

B. H along a hard axis

When a magnetic field is applied along a hard axis, by symmetry one has $\sin^2(2\varphi_1)=\sin^2(2\varphi_2)$ and $\cos(\psi-\varphi_1)=\cos(\psi-\varphi_2)$ ($\psi=\pi/4$), so that also in this case $A_{11}=A_{22}$ and $B_{11}=B_{22}$.

C. H along an easy axis and $H>H_{c1}$

When the magnetic field is applied along an easy axis, and it is greater than the first critical field H_{c1}, the magnetizations of the two coupled layers turn out to be symmetrically disposed with respect to the field direction. Thus, also in this case one has $\sin^2(2\varphi_1)=\sin^2(2\varphi_2)$ and $\cos(\psi-\varphi_1)=\cos(\psi-\varphi_2)$ ($\psi=0$), so that $A_{11}=A_{22}$ and $B_{11}=B_{22}$.

It is worthwhile to mention that, in both cases B and C, a further simplification in the dispersion curve, $B_{12}=0$, occurs when the magnetic field overcomes the critical value for which the two magnetizations of the coupled layers align themselves along the field direction: $H>H_c$ for H along a hard axis; $H>H_{c2}$ for H along an easy axis.

In all the high symmetry cases, for which $A_{11}=A_{22}$ and $B_{11}=B_{22}$, Eq. (22) takes the form [we set $\varepsilon=0$ in Eqs. (18)]

$$\omega_{\rm ac}^2(\mathbf{k}_\parallel)=(A_{11}+A_{12})^2-(B_{11}+B_{12})^2$$
$$=\{4JS[1-\gamma(\mathbf{k}_\parallel)]+g\mu_B H\cos(\psi-\varphi_1)+2KS^3g_s[1-2\sin^2(2\varphi_1)]\}$$
$$\times\{4JS[1-\gamma(\mathbf{k}_\parallel)]+g\mu_B H\cos(\psi-\varphi_1)-AS[1-\cos(\varphi_2-\varphi_1)]+2DSf_s$$
$$+\tfrac{1}{2}BS[(2S-1)^2\cos^2(\varphi_2-\varphi_1)-2(2S^2-2S+1)\cos(\varphi_2-\varphi_1)+1]$$
$$+\tfrac{1}{2}K(2S-1)(2S^2-2S+1)-KS^3g_s\sin^2(2\varphi_1)\}\ , \tag{23a}$$

$$\omega_{\rm op}^2(\mathbf{k}_\parallel)=(A_{11}-A_{12})^2-(B_{11}-B_{12})^2$$
$$=\{4JS[1-\gamma(\mathbf{k}_\parallel)]+g\mu_B H\cos(\psi-\varphi_1)+2AS\cos(\varphi_2-\varphi_1)$$
$$+BS[2(2S-1)^2\cos^2(\varphi_2-\varphi_1)-\cos(\varphi_2-\varphi_1)-(2S-1)^2]+2KS^3g_s[1-2\sin^2(2\varphi_1)]\}$$
$$\times\{4JS[1-\gamma(\mathbf{k}_\parallel)]+g\mu_B H\cos(\psi-\varphi_1)+AS[1+\cos(\varphi_2-\varphi_1)]+2DSf_s$$
$$+\tfrac{1}{2}BS[(2S-1)^2\cos^2(\varphi_2-\varphi_1)+4S(S-1)\cos(\varphi_2-\varphi_1)-1]$$
$$+\tfrac{1}{2}K(2S-1)(2S^2-2S+1)-KS^3g_s\sin^2(2\varphi_1)\}\ . \tag{23b}$$

From the analysis of the eigenvectors of the dynamical matrix $\mathcal{T}(\mathbf{k}_\parallel)$, one can see that the frequency $\omega_{\rm ac}$ corresponds to an acoustic mode, i.e., to an in-phase motion of the spins, whilst $\omega_{\rm op}$ to an optical one, i.e., to an out-of-phase motion. In fact one has $\mathcal{T}\mathcal{U}=\omega_{\rm ac}\mathcal{U}$ and $\mathcal{T}\mathcal{V}=\omega_{\rm op}\mathcal{V}$, where the eigenvectors $\mathcal{U}$ and $\mathcal{V}$ take the form

$$\mathcal{U}=\begin{bmatrix}u_1\\u_1\\u_2\\u_2\end{bmatrix}\ ,\quad \mathcal{V}=\begin{bmatrix}v_1\\-v_1\\v_2\\-v_2\end{bmatrix}\ . \tag{24}$$

IV. RESULTS AND DISCUSSION

In this section we present and discuss the results for the field dependence of the spin-wave frequencies. We suppose the magnetic field to be applied within the film plane along a direction of high symmetry. We limit ourselves to the study of the energy gaps, which in a real system could be measured, e.g., by means of the inelastic Brillouin light-scattering technique.

A. $K=0$ case

Let us first consider the field dependence of the frequencies of the acoustic and optical modes in the limiting case of zero in-plane anisotropy, $K=0$. For zero field, substituting into Eqs. (23) the explicit expression for the canting angle, $\cos(\varphi_2-\varphi_1)=(2A-B)/-4BS^2f_s^2$, one obtains

$$\omega_{ac}^2(\mathbf{k}_\parallel)=\{4JS[1-\gamma(\mathbf{k}_\parallel)]\}\times\{4JS[1-\gamma(\mathbf{k}_\parallel)]+2DSf_s\}\quad(K=0,\ H=0)\ , \tag{25a}$$

$$\omega_{\rm op}^2(\mathbf{k}_\parallel)=\{4JS[1-\gamma(\mathbf{k}_\parallel)]-4BS^3f_s^2[1-\cos^2(\varphi_2-\varphi_1)]\}\times\{4JS[1-\gamma(\mathbf{k}_\parallel)]+2DSf_s\}\quad(K=0,H=0)\ . \tag{25b}$$

It is apparent from Eqs. (23a) and (25a) that the frequency $\omega_{\rm ac}(\mathbf{k}_\parallel)$ of the acoustic mode vanishes for $\mathbf{k}_\parallel\to0$: Such a Goldstone mode is related to an in-phase rotation of the magnetizations of the two coupled layers within the film plane (thus with zero cost in the easy-plane anisotropy D), keeping the canting angle constant (thus with zero cost in the interlayer exchange couplings, A and B).

In contrast, Eq. (25b) shows that the frequency $\omega_{\rm op}(\mathbf{k}_\parallel)$ of the optical mode does not vanish for $\mathbf{k}_\parallel\to0$, in the presence of a finite easy-plane anisotropy D. In fact, this mode is related to an out-of-phase motion of the magnetizations of the two coupled layers, which makes them get out of the film plane in opposite directions; moreover, the in-plane component of the out-of-phase motion causes the canting angle to change linearly in the fluctuations. In the absence of the easy-plane anisotropy $D=0$, also the optical mode would become a Goldstone one, since the two magnetizations would be allowed to fluctuate perpendicularly to the film plane with no cost in D and without change in the canting angle at linear order in the fluctuations, thus with no cost in the interlayer couplings A,B. Clearly, the occurrence of two Goldstone modes for zero field and anisotropies, could have been predicted at the outset, as a consequence of the two continuous symmetries displayed by the Hamiltonian (1) for $D=0$, $K=0$, $H=0$.

The field dependence of the acoustic and optical modes for $\mathbf{k}_\parallel=0$ and zero in-plane anisotropy $K=0$, is displayed in Fig. 4(a). As the field increases, an acoustic spin-wave excitation away from the canted ground state has to overcome two energy barriers: One to deviate from the in-plane field direction and one to move out of the film plane. The first barrier is proportional to H. The second one depends on all the Hamiltonian parameters, but for the set of parameters chosen for Figs. 4 and 5, which are of the correct order of magnitude for describing a real system, such as Fe/Cr/Fe, it is mainly determined by the easy-plane anisotropy D. Thus it results that the frequency of the acoustic mode increases monotonically with increasing H. For $H>H_c$, taking into account that

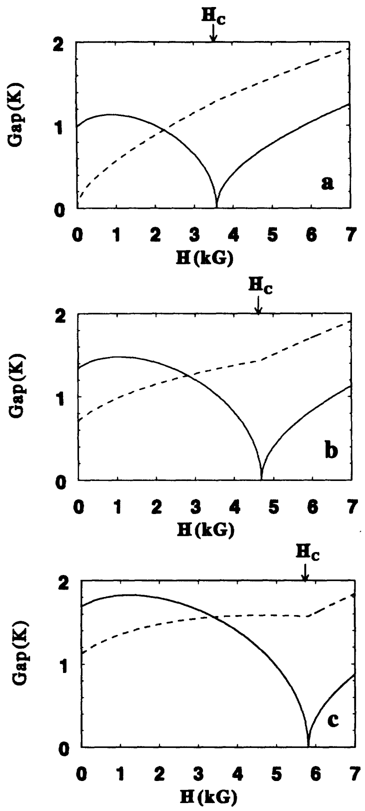

FIG. 4. Field dependence of the acoustic (dashed line) and optical (full line) spin-wave frequencies at zero wave vector, $\mathbf{k}_{\parallel}=0$, for H applied along a hard in-plane axis $\{101\}$, for selected values of the fourfold in-plane anisotropy K: (a) $K=0$; (b) $K=0.10$ K; (c) $K=0.2$ K. The other Hamiltonian parameters are fixed to $A=-0.04$ K; $B=-0.02$ K; $D=1$ K; $S=2$.

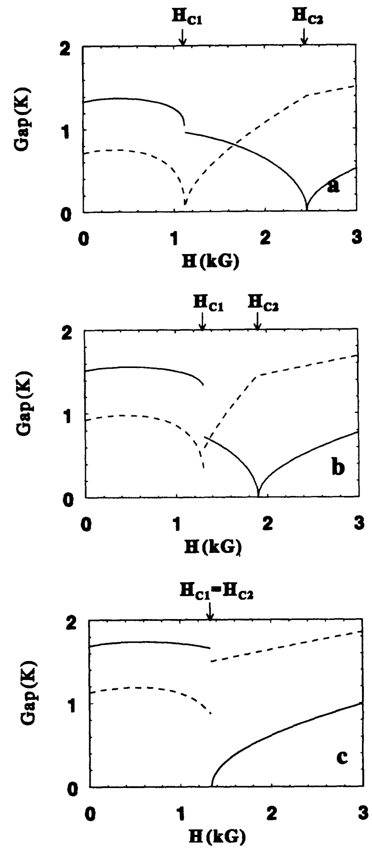

FIG. 5. Field dependence of the acoustic (dashed line) and optical (full line) spin-wave frequencies at zero wave vector, $\mathbf{k}_{\parallel}=0$, for H applied along an easy in-plane axis $\{001\}$, for selected values of the fourfold in-plane anisotropy K: (a) $K=0.10$ K; (b) $K=0.15$ K; (c) $K=0.20$ K. The other Hamiltonian parameters are the same as in Fig. 4.

$\varphi_1=\varphi_2$, $\psi=\pi/4$, one has simply

$$\omega_{ac}(\mathbf{k}_{\parallel}=0)=\sqrt{g\mu_B H(g\mu_B H+2DSf_s)} \quad (K=0,\ H>H_c)\ . \tag{26a}$$

The field dependence of the optical mode is quite different. In this case one can easily show, by substituting Eq. (13) into the second brace on the right-hand side of Eq. (23b), that the energy barrier to move out of the film plane is constant and equal exactly to $2DSf_s$. In contrast, the energy barrier for in-plane deviations from the canted ground state depends on the field. More precisely, upon H approaching H_c, the latter energy barrier decreases (i.e., the system becomes more and more isotropic), until when the field increases further, it constitutes itself an energy barrier. At $H=H_c$, the first brace on the right-hand side of Eq. (23b) vanishes, and so does the gap of the optical mode. For $H>H_c$ one has the simple dependence

$$\omega_{op}(\mathbf{k}_{\parallel}=0)=\sqrt{g\mu_B(H-H_c)[g\mu_B(H-H_c)+2DSf_s]} \quad (K=0\ ,\ H>H_c)\ . \tag{26b}$$

B. General case $K\neq 0$

In Figs. 4(b), 4(c), and 5 we report the dependence of the acoustic and optical frequency gaps on the intensity of a field applied within the film plane, along a hard axis and an easy axis, respectively. First of all, we observe that, in the easy case, the frequency gaps present discontinuous jumps in correspondence to H_{c1}, the critical value of H for which the ground-state configuration undergoes an abrupt change, from a finite value to zero, in the angular variable Γ [see Figs. 3(a), 3(b), 5(a), and 5(b)], or in both Γ and φ_- [see Figs. 3(c) and 5(c)]. We remind the reader that $\Gamma=\varphi_+/2$ denotes the angle formed by the vector sum of the magnetizations of the two coupled layers with the field direction, while φ_- denotes the canting angle.

Common to the hard and easy case is the feature of the vanishing of the optical gap at the saturation field (H_c in the hard case and H_{c2} in the easy case, respectively). This is due to a field-induced mechanism of isotropization of the in-plane motion, similar to the one discussed in the case $K=0$. In contrast, the field dependence of the acoustic mode is quite different in the hard and easy cases.

In the hard case, the acoustic mode presents a monotonic increase with increasing H, as in the $K=0$ case. The only obvious difference is that for $K\neq 0$ also the acoustic mode presents a gap in zero field, since the rotational symmetry within the film plane is broken by the fourfold anisotropy.

In the easy case, a minimum is found also in the field dependence of the acoustic mode, in correspondence to the first critical field H_{c1}, for which the field direction becomes a symmetry axis for the canted ground-state configuration. It should be noted that for $H<H_{c1}$, Eq. (23a) does not hold: One must resort to Eq. (22), thus in this field range it is difficult to understand the dependence of the gap on the Hamiltonian parameters. From Figs. 5(a)–5(c), one can observe that for $H=H_{c1}$ the gap of the acoustic mode increases with increasing K, suggesting that the minimum is probably due to an incomplete compensation between the field and the in-plane anisotropy K.

V. CONCLUSIONS

We have investigated, within a microscopic and quantum approach, the ground-state configuration and the spin-wave excitations of a model of two ferromagnetic monolayers coupled by bilinear and biquadratic exchange, in the presence of a field applied in plane along a high-symmetry direction.

For the $H=0$ phase diagram, with respect to the classical case,[5] we have found some modifications in the phase boundaries owing to the inclusion of quantum corrections. For the applied field, we have calculated the mean of the $T=0$ magnetizations of the two coupled layers versus H, for selected values of the in-plane anisotropy. Such $M(H)$ curves present changes in slope at the saturation field, where the canting angle φ_- goes to zero; also, in the easy-axis case, $M(H)$ exhibits a discontinuity at the same field as Γ.

Using a Green's-function method, we have calculated the spin-wave frequencies of the system in analytic form. Minima are found in the field dependence of the acoustic and optical frequency gaps, in correspondence to the aforementioned critical fields. The calculated minima have been attributed to a field-induced mechanism of isotropization of the system within the easy plane. We suggest that they could be experimentally observed by Brillouin light scattering in sandwich structures made of ultrathin ferromagnetic films separated by a nonmagnetic spacer, provided that (a) the intraplane interaction is much greater than the interlayer ones and (b) domain effects are fairly unimportant (i.e., provided that the multidomain state observed in Ref. 5 is a very unstable intermediate state between monodomain stable configurations,[6] with respect to which the spin-wave excitations are calculated). Both conditions seem to be satisfied in the case of Fe/Cr/Fe, Fe/Al/Fe, and Fe/Au/Fe.[29] In the end, the fact that the discontinuities in the gap of the optical mode are very large and strongly dependent on A and B, makes possible the experimental determination of the above parameters.

Note added in proof. After submission of this manuscript, the experimental paper by B. Rodmacq *et al.* [Phys. Rev. B **48**, 3556 (1993)] had been published. The authors revealed a crossover from a canted state at low temperature to an antiferromagnetic one beyond 100 K in $Ni_{81}Fe_{19}/Ag$ multilayers, owing to the temperature dependence of the biquadratic exchange. This fact led us to investigate the spectrum of the magnetic excitations with respect to the antiferromagnetic ground state in the presence of bilinear and biquadratic exchange. See: M. Macciò, M. G. Pini, P. Politi, and A. Rettori, in *Proceedings of the 38th MMM Conference, Minneapolis, Minnesota, 1993* [J. Appl. Phys. (to be published)].

ACKNOWLEDGMENT

Fruitful discussions with U. Balucani are gratefully acknowledged.

APPENDIX

Here we report the analytic expressions for the boundary lines in the zero-field phase diagram (see Fig. 1)

$$f_0(\alpha)=2\alpha,\quad \forall\alpha\ , \tag{A1}$$

$$f_1(\alpha)=\frac{-1+2\alpha}{(2S-1)^2+1}\ ,\quad \text{for } \alpha<0\ , \tag{A2a}$$

$$f_1(\alpha)-\frac{-1-2\alpha}{(2S-1)^2-1}\ ,\quad \text{for } \alpha>0\ , \tag{A2b}$$

$$f_2(\alpha)=\frac{2\alpha}{(2S-1)^2+1}+\frac{(2S-1)^2+2}{2[(2S-1)^2+1]} -\left[\frac{[(2S-1)^2+2]^2}{4[(2S-1)^2+1]^4}-\frac{2\alpha(2S-1)^2}{[(2S-1)^2+1]^3}\right]^{1/2},\quad \text{for } \alpha<0\ , \tag{A3a}$$

$$f_2(\alpha)=-\frac{2\alpha}{(2S-1)^2-1}+\frac{(2S-1)^2-2}{2[(2S-1)^2-1]} -\left[\frac{[(2S-1)^2-2]^2}{4[(2S-1)^2-1]^4}+\frac{2\alpha(2S-1)^2}{[(2S-1)^2-1]^3}\right]^{1/2},\quad \text{for } \alpha>0\ , \tag{A3b}$$

$$f_3(\alpha)=-\frac{4\alpha+\sqrt{8\alpha^2(2S-1)^4+(2S-1)^4-2}}{(2S-1)^4-2}\ , \quad \forall\alpha\ . \tag{A4}$$

[1] P. Grünberg, R. Schreiber, Y. Pang, M. B. Brodsky, and H. Sowers, Phys. Rev. Lett. **57**, 2442 (1986).

[2] S. S. P. Parkin, N. More, and K. P. Roche, Phys. Rev. Lett. **64**, 2304 (1990).

[3] J. Unguris, R. J. Celotta, and D. T. Pierce, Phys. Rev. Lett. **67**, 140 (1991).

[4] S. Demokritov, J. A. Wolf, and P. Grünberg, Europhys. Lett. **15**, 881 (1991).

[5] M. Rürigh, R. Schäfer, A. Hubert, R. Mosler, J. A. Wolf, S. Demokritov, and P. Grünberg, Phys. Status Solidi A **125**, 635 (1991).

[6] U. Köbler, K. Wagner, R. Wiechers, A. Fuss, and W. Zinn, J. Magn. Magn. Mater. **103**, 236 (1992).

[7] J. Barnaś and P. Grünberg, J. Magn. Magn. Mater. **82**, 186 (1989).

[8] B. Heinrich, Z. Celinski, F. Cochran, A. S. Arrott, K. Myrtle, and S. T. Purcell, Phys. Rev. B **47**, 5077 (1993).

[9] Y. Yafet, Phys. Rev. B **36**, 3948 (1987).

[10] Y. Wang, P. M. Levy, and J. L. Fry, Phys. Rev. Lett. **65**, 2732 (1990); J. L. Fry, E. C. Etheridge, P. M. Levy, and Y. Wang, J. Appl. Phys. **69**, 4780 (1991).

[11] P. Bruno and C. Chappert, Phys. Rev. Lett. **67**, 1602 (1991); **67**, 2592(E) (1991); Phys. Rev. B **46**, 261 (1992).

[12] D. M. Edwards, J. Mathon, R. B. Muniz, and M.S. Phan, Phys. Rev. Lett. **67**, 493 (1991); J. Phys. Condens. Matter **3**, 4941 (1991).

[13] J. Mathon, J. Magn. Magn. Mater. **100**, 527 (1991).

[14] R. Coehoorn, Phys. Rev. B **44**, 9331 (1991).

[15] J. C. Slonczewski, Phys. Rev. Lett. **67**, 3172 (1991).

[16] R. Ribas and B. Dieny, Phys. Lett. A **167**, 103 (1992).

[17] J. Barnaś and P. Grünberg, J. Magn. Magn. Mater. **121**, 326 (1993).

[18] J. Barnaś, J. Magn. Magn. Mater. **123**, L21 (1993).

[19] For a general review about biquadratic coupling, see E. L. Nagaev, Usp. Fiz. Nauk **136**, 61 (1982) [Sov. Phys. Usp. **25**, 31 (1982)].

[20] See F. Keffer, in *Handbuch der Physik,* edited by S. Flugge (Springer, Berlin, 1966), Vol. XVIII/B.

[21] It is useful to remind the reader of the relation between different notations (G = Grünberg): $AS^2=A_{12}^{(G)}$, $BS^4=2B_{12}^{(G)}$, $KS^4=K^{(G)}$.

[22] It is worthwhile to note that in Fig. 1 such effects are enhanced by an opportune choice of axis scales, which are different from those used in Ref. 5.

[23] An example of the phase diagram of two films, coupled by both bilinear and biquadratic exchange, in presence of a field can be found in Ref. 6.

[24] U. Balucani, M. G. Pini, A. Rettori, and V. Tognetti, J. Phys. C **13**, 3895 (1980).

[25] In fact in Eq. (18a) one has for $\varepsilon=1$: $(-4S^2+7S-4)+(3S-2)=-2(S-1)(2S-3)$.

[26] E. Rastelli and A. Tassi, J. Phys. C **17**, 727 (1984).

[27] S. Goldstone, Nuovo Cimento **19**, 154 (1961); R. V. Lange, Phys. Rev. **146**, 301 (1966).

[28] P. Politi, M. G. Pini, and A. Rettori, Phys. Rev. B **46**, 8312 (1992).

[29] A. Fuss, S. Demokritov, P. Grünberg, and W. Zinn, J. Magn. Magn. Mater. **103**, L221 (1992).